BIOCHEMISTRY
including biophysical chemistry & molecular biology

Article

pubs.acs.org/biochemistry

Probing Minor Groove Hydrogen Bonding Interactions between RB69 DNA Polymerase and DNA

Shuangluo Xia, Thomas D. Christian, Jimin Wang, and William H. Konigsberg*

Department of Molecular Biophysics and Biochemistry, Yale University, New Haven, Connecticut 06520-8114, United States

Supporting Information

ABSTRACT: Minor groove hydrogen bonding (HB) interactions between DNA polymerases (pols) and N3 of purines or O2 of pyrimidines have been proposed to be essential for DNA synthesis from results obtained using various nucleoside analogues lacking the N3 or O2 contacts that interfered with primer extension. Because there has been no direct structural evidence to support this proposal, we decided to evaluate the contribution of minor groove HB interactions with family B pols. We have used RB69 DNA pol and 3-deaza-2′-deoxyadenosine (3DA), an analogue of 2-deoxyadenosine, which has the same HB pattern opposite T but with N3 replaced with a carbon atom. We then determined pre-steady-state kinetic parameters for the insertion of dAMP opposite dT using primer/templates (P/T)-containing 3DA. We also determined three structures of ternary complexes with 3DA at various positions in the duplex DNA substrate. We found that the incorporation efficiency of dAMP opposite dT decreased 10^2−10^3-fold even when only one minor groove HB interaction was missing. Our structures show that the HB pattern and base pair geometry of 3DA/dT is exactly the same as those of dA/dT, which makes 3DA an optimal analogue for probing minor groove HB interactions between a DNA polymerase and a nucleobase. In addition, our structures provide a rationale for the observed 10^2−10^3-fold decrease in the rate of nucleotide incorporation. The minor groove HB interactions between position $n - 2$ of the primer strand and RB69pol fix the rotomer conformations of the K706 and D621 side chains, as well as the position of metal ion A and its coordinating ligands, so that they are in the optinal orientation for DNA synthesis.

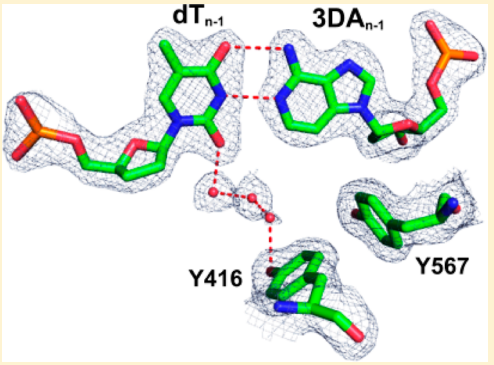

DNA polymerases are essential for the maintenance of genetic integrity with reported error frequencies for replicative DNA polymerases (pols) that are typically $<10^{-6}$ for every insertion event.[1−5] Several factors that contribute to the high level of base selectivity have been identified; these include base stacking, base pair geometry, and interbase hydrogen bonding (HB).[6−8] In addition, minor groove HB interactions between the nucleobases in the DNA duplex and the pol contribute to the efficiency of DNA synthesis and base selectivity.[9−13] The lone pair of electrons carried by N3 in standard purines or O2 in standard pyrimidines are competent HB acceptors that can interact with HB donors presented by the pols.[14] Indeed, structures of various pols from different families have provided direct evidence of pol−minor groove HB interactions.[11,15−19] In family A pols, a conserved Arg residue forms a HB to N3 or O2 of the nucleobase at position $n - 1$ (in both the primer and template strands).[18−20] Similarly, in family B pols, a conserved Tyr residue forms a HB with the nucleobase at position $n - 1$ of the template strand in the minor groove via a water molecule.[11,21] Single-site mutagenesis showed that substitution of certain highly conserved residues (Arg in family A pols or Lys in family B pols) with Ala dramatically reduced the catalytic efficiency.[22−25] Further evidence of the role of minor groove−pol HB interactions in enhancing the efficiency of DNA synthesis have come from experiments that employed nucleotide analogues lacking either an N3 atom in purines or an O2 atom in pyrimidines. For example, Morales et al.[26] used non-HB nucleoside isosteres, 9-methyl-1*H*-imidazo[4,5-*b*]-pyridine (Q), 4-methylbenzimidazole (Z), and difluorotoluene (F), to probe the role of minor groove HB interactions with the Klenow fragment (KF). They concluded that minor groove HB interactions are more important for primer extension than for insertion of base analogues.[13,26] However, there was no direct structural evidence to support this contention or to exclude other possibilities that could account for the reduction in incorporation efficiency, such as unforeseen properties of these nucleotide analogues. Our kinetic and structural studies using DNA with an abasic site in the templating position demonstrated that base stacking between an incoming dNTP and base-pairs at position $n - 1$ plays an important role in the efficiency of nucleotide incorporation.[27] Introducing a nucleoside isostere incapable of HB with bases either in the primer or in the template strand at position $n - 1$ might have been expected to affect base stacking of the incoming dNTP. In addition, our recently reported structures of the ternary complex of RB69 DNA polymerase (RB69pol) containing F in the templating position showed that F can form HBs with

Received: April 2, 2012
Revised: May 4, 2012
Published: May 9, 2012

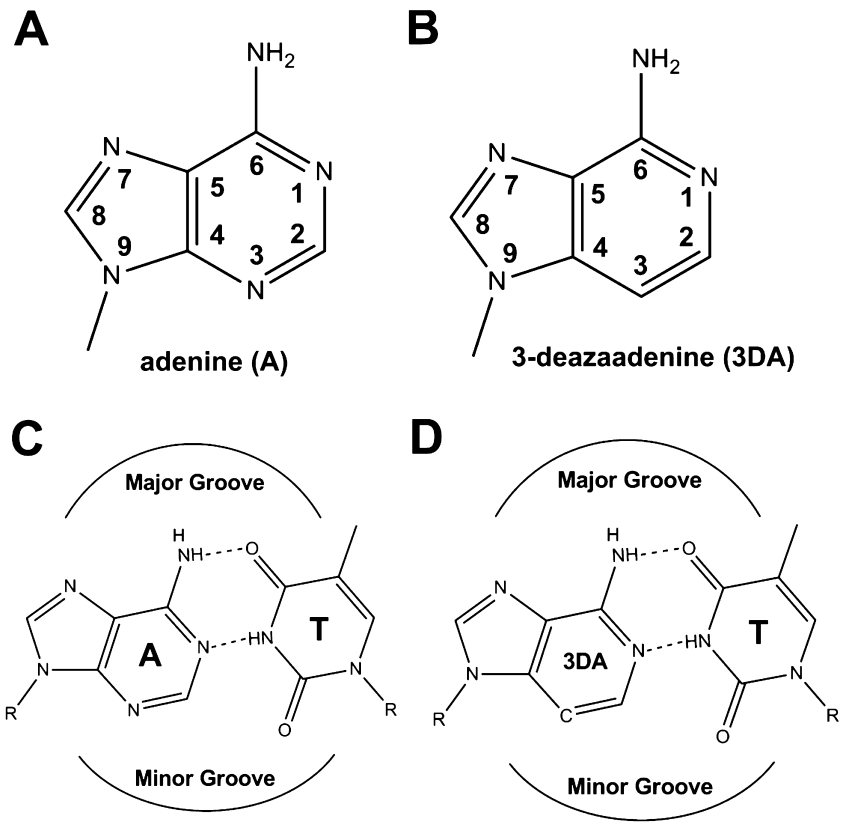

Figure 1. Chemical structure and hydrogen bonding pattern of 3DA. (A) Chemical structure of adenine. (B) Chemical structure of 3DA. (C) Complementary dA/dT base pair. (D) 3DA/dT base pair.

incoming dNTPs directly or indirectly via water molecules.[28,29] We decided to revisit this important issue regarding the role of minor groove HBs using RB69 DNA pol (RB69pol) and 3-deaza-2′-deoxyadenosine (3DA), an analogue of 2-deoxyadenosine (dA) in which N3 is replaced with a carbon atom. 3DA has the same hydrogen bonding pattern with dT as does dA, making it an ideal analogue for use as a probe to study these interactions (Figure 1).

We chose RB69pol as a representative of B family pols because it is extensively similar in sequence to human and other eukaryotic replicative DNA pols.[30] In addition, there is a wealth of structural and kinetic data available that would be expected to aid in the interpretation of results obtained with this enzyme.[11,31−37] The structure of the dCTP/dG-containing ternary complex of RB69pol at 1.8 Å resolution has shown that (i) Y567 forms a HB with N3 of G at position $n - 1$ of the template strand via a water molecule and (ii) K706 forms a HB with N3 of A at position $n - 2$ of the primer strand.[35] Both Y567 and K706 are highly conserved residues in family B pols.[30] To assess whether RB69pol employs minor groove hydrogen bond interactions as one of the ways that RB69pol, and likely other pols, optimize substrate binding and reactive center alignment, we examined the efficiency of incorporation of correct incoming nucleotides into DNA that had 3DA at positions $n - 1$, $n - 2$, and $n - 3$ in the primer strand and at position $n - 1$ in the template strand. Our pre-steady-state kinetic data showed that minor groove HB interactions are essential for DNA synthesis. Missing just one minor groove HB interaction resulted in a nearly 10^3-fold decrease in catalytic efficiency for insertion of dAMP opposite dT. We also determined three structures of dATP/dT-containing ternary complexes: one with wt RB69pol and control DNA without 3DA, a second with a P/T that had 3DA at position $n - 1$ in the template strand, and a third with a P/T that had 3DA at position $n - 3$ in the primer strand. These structures provide a basis for understanding why the absence of one minor groove HB interaction with a pol resulted in a 10^2−10^3-fold decrease in the efficiency of nucleotide incorporation.

EXPERIMENTAL PROCEDURES

Chemicals. All chemicals were of the highest quality commercially available; dNTPs were purchased from Roche (Roche Applied Science, Indianapolis, IN). T4 polynucleotide kinase was purchased from New England BioLabs (Boston, MA). [γ-^{32}P]ATP was purchased from MP Biomedicals (Irvine, CA).

Enzymes. wt RB69pol and the Y567A mutant RB69pol, in an exonuclease-deficient background (D222A and D327A), were overexpressed in *Escherichia coli* strain BL21(DE), purified, and stored as previously described.[35,37,38]

DNA Substrates. All oligonucleotides were synthesized at the Keck facilities (Yale University) and purified via polyacrylamide gel electrophoresis (PAGE). The sequence of the primer/template (P/T) used in this study is shown in Figure 2. For kinetic studies, the primer was labeled on the 5′-end with ^{32}P using T4 polynucleotide kinase and [γ-^{32}P]ATP and annealed to the corresponding templates as previously described.[34,35,37] For crystallization, ddT- or ddC-terminated primers were used to prevent phosphoryl transfer.

Chemical Quench Experiments. Rapid chemical quench experiments were performed at 23 °C using a KinTek RFQ-3 instrument (KinTek Corp., University Park, PA). Each reaction

dx.doi.org/10.1021/bi300416z | *Biochemistry* 2012, 51, 4343−4353

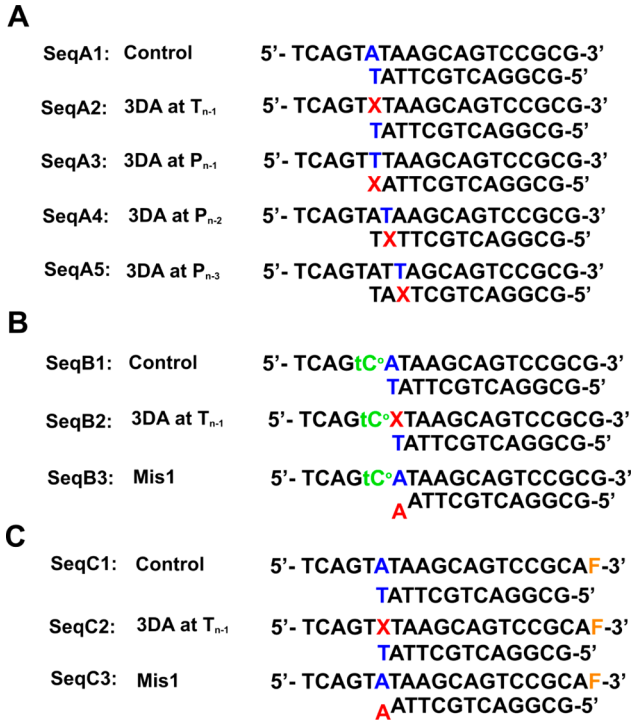

Figure 2. P/T sequences used in this study. (A) P/T sequences used in chemical quench experiments. (B) P/T sequences used in fluorescence lifetime experiments. (C) P/T sequences used in fluorescence anisotropy experiments. Here X stands for 3DA, and F stands for fluorescein.

mixture contained 66 mM Tris-HCl (pH 7.4) and 10 mM $MgSO_4$. All experiments were performed under single-turnover conditions, with a 10-fold excess of RB69pol over the P/T. The concentrations of enzyme after mixing were 1 μM, and the P/T concentration was 83 nM. Products were separated by 19:1% (w/v) PAGE containing 8 M urea, imaged on an MD Strom 860 imager (Molecular Imaging), and quantified using ImageQuaNT. For each $K_{d,app}$ and k_{pol} determination, seven different dNTP concentrations were used. Data from the single-turnover experiments were fit to a single-exponential equation as previously described.[34,35,37] The corresponding standard deviations were calculated from data fitting using Grafit5.0 (Erithacus Inc.).

Determination of Dissociation Constants for RB69pol−P/T Binary Complexes. Fluorescence anisotropy experiments were performed as previously described.[37] The binding buffer contained 50 mM Tris-HCl (pH 7.4) and 10 mM $MgSO_4$. All experiments were performed in duplicate.

Fluorescence Lifetime Determinations. These experiments were conducted as described previously except that tC° was used in place of 2AP.[39] The excitation and emission wavelengths for tC° are 364 and 450 nm, respectively. The final reaction mixtures consisted of 50 mM Tris (pH7.4), 10 mM $MgSO_4$, 200 nM P/T, and 4 μM RB69pol. The methods and data analysis were the same as those described previously.[39]

Crystallization of dATP/dT-Containing wt RB69pol Ternary Complexes. Wild-type RB9pol was mixed in an equimolar ratio with a dideoxy-terminated P/T to give a final protein concentration of 120 μM. dATP was then added to give a final concentration of 2 mM. Crystals were grown under silicon oil using a microbatch procedure.[28,29,35−38] A solution

Table 1. Crystallographic Statistics for Data Collection and Structure Refinement of dATP/dT-Containing Ternary Complexes of wt RB69pol[a]

	control	3DA at $n-1$ (T)	3DA at $n-3$ (P)
space group	$P2_12_12_1$	$P2_12_12_1$	$P2_12_12_1$
unit cell dimensions a, b, c (Å)	74.98, 119.83, 129.95	74.64, 120.18, 130.67	78.14, 119.50, 130.54
resolution range (Å)	50.0−2.15 (2.23−2.15)	50.0−2.02 (2.09−2.02)	50.0−2.31 (2.39−2.31)
no. of unique reflections	63686	76820	55522
redundancy	4.4 (3.8)	4.0 (4.0)	4.8 (4.9)
completeness (%)	99.2 (99.7)	99.4 (99.8)	99.9 (100.0)
R_{merge}[b] (%)	13.5 (95.8)	10.5 (93.2)	7.6 (96.0)
I/σ	11.3 (1.2)	12.7 (1.1)	16.8 (1.3)
final model (no.)			
amino acid residues	903	903	903
water molecules	354	537	187
metal ions	5	5	5
template nucleotides	18	18	18
primer nucleotides	13	13	13
dNTP molecules	1	1	1
Refinement Statistics			
no. of reflections	60252	72694	52490
R_{work}[c] (%)	19.7 (25.7)	19.0 (32.4)	20.8 (26.5)
R_{free}[c] (%)	24.4 (31.6)	22.6 (35.9)	25.9 (33.5)
rmsd[d]			
bond lengths (Å)	0.009	0.008	0.007
bond angles (deg)	1.190	1.165	1.149
PDB entry	4DU1	4DU3	4DU4

[a]Statistics for the highest-resolution shell are given in parentheses. [b]$R_{merge} = \sum_{hkl}\sum_j|I_j(hkl) - \langle I(hkl)\rangle|/\sum_{hkl}\langle I(hkl)\rangle$; statistics for merging all observations for given reflections. [c]$R = \sum_{hkl}|F_{obs}(hkl) - F_{calc}(hkl)|/\sum_{hkl}F_{obs}(hkl)$; statistics for crystallographic agreement between the measured and model-calculated amplitudes. R_{free} is the agreement for the cross-validation data set. [d]Root-mean-square-deviations from ideal values.

dx.doi.org/10.1021/bi300416z | Biochemistry 2012, 51, 4343−4353

Table 2. Pre-Steady-State Kinetic Parameters for Incorporation of dAMP Opposite dT by wt and Y567A RB69pol[a]

RB69pol	P/T[b]	P/T details	k_{pol} (s^{-1})	$K_{d,app}$ (μM)	k_{pol}/K_d (μM^{-1} s^{-1})	ratio
wt	SeqA1	control	296	36	8.2	
wt	SeqA2	3DA at $n-1$ (T)	61	665	9.1×10^{-2}	1/90
wt	SeqA3	3DA at $n-1$ (P)	38	670	5.7×10^{-2}	1/144
wt	SeqA4	3DA at $n-2$ (P)	10	1100	9.1×10^{-3}	1/901
wt	SeqA5	3DA at $n-3$ (P)	293	38	7.7	1/1.1
Y567A	SeqA1	control	290	40	7.2	
Y567A	SeqA2	3DA at $n-1$ (T)	283	42	6.7	1.0

[a]The standard deviation for the $K_{d,app}$ values was ±15%. The standard deviation for the k_{pol} values was ±10%. Representative gels, progress curves, and plots of k_{obs} vs dATP concentration with SeqA1 and SeqA2 are shown in Figure S1 of the Supporting Information. [b]Sequence of P/Ts are shown in Figure 2A.

containing 120 mM $CaCl_2$, 12% (w/v) PEG 350 monomethyl ether (MME), and 100 mM sodium cacodylate (pH 6.5) was mixed with an equal volume of the protein complex. The square rod-shaped crystals grew in 2 days at 20 °C and had typical dimensions of ~150 μm × 70 μm × 70 μm. Crystals were transferred from the mother liquor to a cryoprotectant solution with the same components but containing a high concentration of PEG 350 MME (30%, w/v) prior to being frozen in liquid nitrogen.

Data Collection, Structure Determination, and Refinement. X-ray diffraction data were collected using the synchrotron radiation sources at beamline 24ID-E [Northeast Collaborative Access Team (NECAT), Advanced Photon Source, Argonne National Laboratory, Chicago, IL]. The data were processed using HKL2000 (Table 1 and Table S1 of the Supporting Information).[40] The structures were determined by molecular replacement using Phaser,[41] starting with the wt RB69pol structure of the ternary complex [Protein Data Bank (PDB) entry 3NCI], and refined using REFMAC5.[42] The P/T duplex and dNTP were built using COOT.[43] Structure refinement statistics are listed in Table 1 and Table S1 of the Supporting Information. All figures were made using Pymol.[44]

PDB Entries. Coordinates and structure factors for the dATP/dT-containing wt RB69pol ternary complex structure have been deposited in the Protein Data Bank as entries 4DU1 (with control DNA), 4DU3 (with 3DA at position $n-1$ of the template strand), and 4DU4 (with 3DA at position $n-3$ of the primer strand). In addition, coordinates and structure factors for the dQTP/dT-containing ternary complex of the RB69pol triple mutant were deposited as PDB entry 4E3S.

RESULTS AND DISCUSSION

Incorporation of dAMP into DNA Containing 3DA at Different Positions in the P/T. To determine the precise role of HB interactions between RB69pol and the minor groove in a P/T duplex, we designed P/Ts with 3DA at position $n-1$, $n-2$, or $n-3$ in the primer strand or at position $n-1$ in the template strand (Figure 2A). As shown in Figure 1, substitution of nitrogen with carbon eliminates the possibility of HB between position 3 of adenine and the pol while the overall geometry and W–C HB capability between the incoming dATP and the templating thymine remain unchanged. Thus, any variation in the kinetic parameters, e.g., k_{pol} or $K_{d,app}$ for insertion of dAMP opposite dT, resulting from the dA to 3DA substitution can be ascribed to the disruption of the critical HB interaction between pol and position 3 of the adenine residue in the P/T duplex. Under pre-steady-state conditions, the efficiency of incorporation of dAMP opposite dT by wt RB69pol varies markedly depending on the position of 3DA in the duplex. As shown in Table 2, substitution of dA with 3DA at position $n-1$ of the template strand results in a 5-fold decrease in k_{pol} and an 18-fold increase in $K_{d,app}$. The change is even more dramatic when the 3DA substitution is in the primer strand. Replacing dA with 3DA at position $n-1$ of the primer strand causes the catalytic efficiency to decrease by 144-fold. When 3DA is at position $n-2$ in the primer strand, the k_{pol} and $K_{d,app}$ values for incorporation of dAMP opposite dT were 10 s^{-1} and 1100 μM, respectively, which are almost 30-fold lower for k_{pol} and 30-fold higher for $K_{d,app}$, resulting in a 900-fold decrease in catalytic efficiency compared to the kinetic parameters obtained with control DNA. Interestingly, replacing dA with 3DA at position $n-3$ of the template strand did not affect k_{pol} and $K_{d,app}$ values for incorporation of dAMP opposite dT. Therefore, some minor groove–pol HB interactions are not essential for nucleotide incorporation.

The structure that we have reported for a dATP/dT-containing ternary complex of Y567A RB69pol shows that the minor groove HB network at position $n-1$ of the template strand and the pol was disrupted by replacing Y567 with Ala.[37,39] It is very likely that the Y567A RB69pol mutant was not able to sense the dA to 3DA substitution at this position. As predicted, the kinetic parameters for incorporation of dAMP opposite dT by the Y567A RB69pol mutant were almost identical for both control DNA and DNA with 3DA at position $n-1$ of the template strand (Table 2).

Determination of Fluorescence Lifetimes. To determine the effect of HB interactions between RB69pol and the minor groove of the P/T duplex in partitioning the DNA substrate between the pol and exo domains, we designed three duplex DNAs with tC°, an analogue of dC, at position n of the template strand (Figure 3). At position $n-1$, the first duplex (Figure 2B, SeqB1) has a normal W–C dT/dA base pair; the second (Figure 2B, SeqB2) has a dT/3DA base pair, and the third (Figure 2B, SeqB3) has an dA/dA mismatched base pair. The lifetime of tC° fluorescence depends largely on its local environment.[45,46] We assume that, in a pol–P/T binary complex, the majority of SeqB1 will be in the pol domain and the majority of SeqB3 will be in the exo domain. If minor groove HB interactions are important for keeping a P/T in the pol domain, then the local environment of tC° in SeqB2 will resemble that of tC° in SeqB1; otherwise, it will be closer to that of tC° in SeqB3. As shown in Table 3, a single fluorescent species with a 3.8–3.9 ps fluorescence lifetime was observed for duplex DNA SeqB1 and SeqB2. When tC° binds RB69pol, the fluorescence intensity of tC° increases, as does the fluorescence lifetime. Three fluorescent species with 4.3 ns, 6.4 ns, and 39 ps fluorescence lifetimes were observed for the pol–SeqB1 (control DNA) binary complex. The existence of multiple

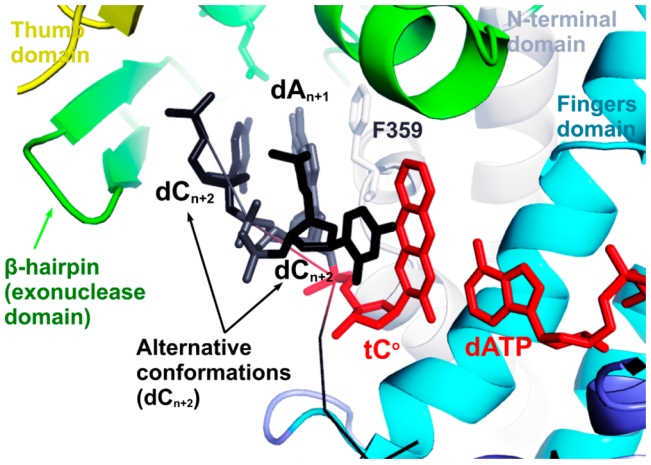

Figure 3. Two alternative conformations of the 5′-overhang of template strand DNA in the dATP- and tC°-containing ternary complex of Y567A RB69pol. The chemical structure of tC° is shown in Figure S3 of the Supporting Information.

fluorescent species is consistent with our recently reported dATP- and tC°-containing ternary complex of Y567A RB69pol.[47] The 5′-overhang of the template strand has two alternative conformations; the base of dC at position $n + 2$ of the template strand can either stack between the β-hairpin and the dA base at position $n + 1$ in the template strand or flip backward forming a Hoogsteen base pair with dG at position $n - 1$ of the template strand (Figure 3). The β-hairpin in the exonuclease domain of RB69pol acts as a wedge to separate the end of the primer strand from the template. Thus, a conformational change involving the β-hairpin will affect the local environment of tC° at position n when the 3′-end of the primer partitions into the exonuclease domain. Replacing dA with 3DA at position $n - 1$ of the template strand affects fluorescence lifetimes as follows. (i) The amplitudes of the two nanosecond lifetime species decrease by 30% (Table 3). (ii) The amplitude of the picosecond lifetime species increases by 50% (Table 3). (iii) The value of the lifetime for the picosecond lifetime species decreases by 40% (Table 3). Thus, the local environment of tC° in SeqB2 is not exactly the same as that of tC° in SeqB1. By replacing a normal W−C base pair with a dA/dA mismatch, the amplitude for the picosecond species increases by 75% and the lifetime of the picosecond species decreases by 50%. By comparison, the values and amplitudes of fluorescence lifetimes of tC° in SeqB2 are closer to those of SeqB3 than those of SeqB1. Clearly, pol−minor groove HB interactions help to stabilize the P/T in the pol domain.

Determination of RB69pol-P/T Dissociation Constants. A concern raised by the results of the fluorescence lifetime measurements is whether minor groove HB interactions affect the dissociation of pol−P/T binary complexes. We tested this using fluorescence anisotropy. As shown in Table 4, the K_d for the wt RB69pol with control DNA is 152 nM. Substitution of dA with 3DA at position $n - 1$ of the template strand in the DNA duplex did not affect the corresponding binding affinity for RB69pol as the two K_d values are almost identical (Table 4). Thus, the increase in $K_{d,app}$ values observed with 3DA at position $n - 1$, determined using single-turnover conditions, was mainly due to substrate misalignment and a sparser population of the pol−P/T binary complex in the pol mode. In addition, replacing dA/dT with dA/dA at the position $n - 1$ of the P/T duplex did not affect the binding affinity of pol for the P/T duplex (Table 4). Therefore, the change in the fluorescence lifetime of tC° in SeqB3 is due to the partitioning of the primer strand from the pol to the exo domain.

Table 4. Ground-State Dissociation Constants of RB69pol−P/T Binary Complexes[a]

P/T[b]	P/T details	K_d (nM)
SeqC1	control	152
SeqC2	3DA at $n - 1$ (T)	156
SeqC3	dA/dA at $n - 1$	150

[a]The standard deviation for the K_d values was ±25%. [b]Sequences of P/Ts are shown in Figure 2C.

Structural Studies of the dATP/dT-Containing Ternary Complex of Wild Type RB69pol with 3DA at Various Positions in the DNA Duplex. In an attempt to provide a structural basis that could account for the 10^2−10^3-fold difference in incorporation efficiency when 3DA was substituted for dA in various positions of the P/T, we determined the crystal structures of three dATP/dT-containing ternary complexes of wt RB69pol that differed as follows. One contained control duplex DNA; the second had 3DA at position $n - 1$ in the template strand of the P/T, and the third had 3DA at position $n - 3$ in the primer strand of the P/T. These three structures were determined with resolutions ranging from 2.02 to 2.31 Å and R_{free} values ranging from 22.6 to 25.9%. The overall structures of all three ternary complexes were identical to that of our reported 1.8 Å dCTP/dG-containing wt RB69pol ternary complex with root-mean-square deviations of Cα atoms varying from 0.18 to 0.21 Å.[35] The electron densities for the P/T duplex DNA and the surrounding network of ordered water molecules are well-defined in the structures reported here (Figure 4).

Table 3. Fluorescence Lifetimes of tC° in Duplex DNA and the pol−P/T Binary Complex[a]

RB69pol	P/T[b]	P/T details	τ_1 (ns)	τ_2 (ns)	τ_3 (ps)	χ^2
	SeqB1	control			3.8 (1.0)	1.04
	SeqB2	3DA at $n - 1$ (T)			3.9 (1.0)	0.98
wt	SeqB1	control	4.3 (0.29)	6.4 (0.34)	39 (0.37)	1.05
wt	SeqB2	3DA at $n - 1$ (T)	4.3 (0.19)	7.6 (0.25)	23 (0.56)	1.03
wt	SeqB3	dA/dA at $n - 1$	4.3 (0.19)	7.0 (0.16)	19 (0.65)	1.07

[a]The standard deviation for the lifetime values was ±15%. The numbers in parentheses are the corresponding amplitudes for the lifetime species. Representative fluorescence decay of wt RB69pol with SeqB2 shown in Figure S2 of the Supporting Information. [b]Sequences of P/Ts are shown in Figure 2B.

dx.doi.org/10.1021/bi300416z | Biochemistry 2012, 51, 4343−4353

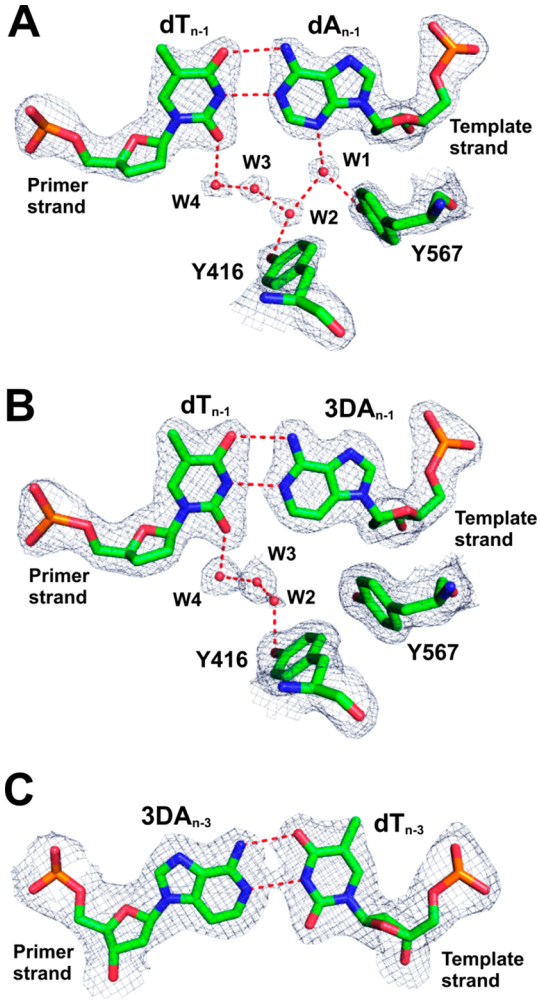

Figure 4. Structures of base pairs at positions $n - 1$ and $n - 3$ of the P/T. (A) Final $2F_o - F_c$ electron density map for the wt RB69pol with control DNA contoured at 1.8σ. (B) Final $2F_o - F_c$ electron density map for the wt RB69pol with 3DA at position $n - 1$ of the template strand contoured at 1.2σ. (C) Final $2F_o - F_c$ electron density map for the wt RB69pol with 3DA at position $n - 3$ of the primer strand contoured at 1.2σ.

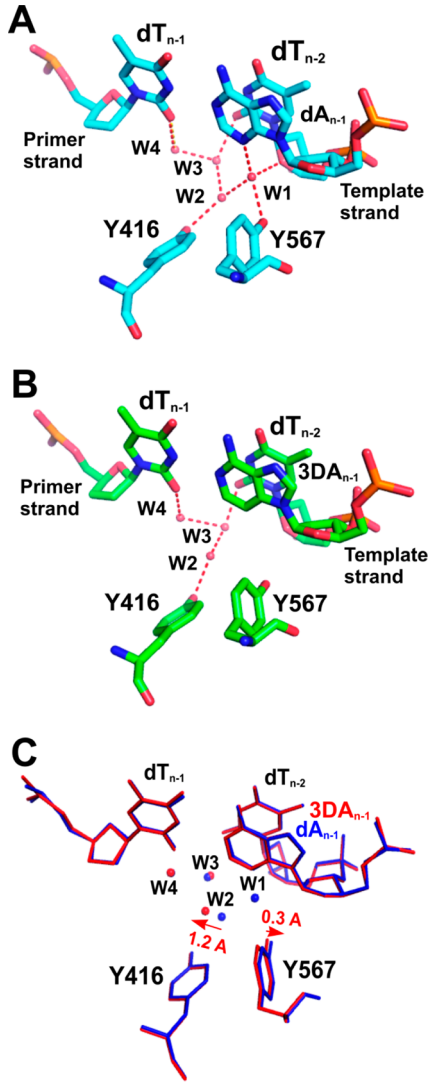

Figure 5. Minor groove HB at position $n - 1$. (A) Overview of the NBP of wt RB69pol with control DNA. A rigid HB network with ordered water molecules labeled W1–W4 contacts the minor groove of the P/T DNA duplex. (B) Overview of the NBP of wt RB69pol with 3DA at position $n - 1$ of the template strand. (C) Superposition of panels A (shown as blue sticks) and B (shown as red sticks).

Consistent with our previous findings, a rigid HB network involving the γ-OH groups of Y567, Y416, and five ordered water molecules (four of them shown in Figure 5A) was observed in the minor groove of the nascent P/T duplex in our structure containing control DNA. As shown in Figure 5A, the W1 water molecule was in perfect tetrahedral coordination. It formed a HB with N3 of dA at position $n - 1$ of the template strand. The HB distance between W1 and N3 was 2.69 Å. The adjacent W2 water molecule was in an unusual planar trigonal geometry, a feature that was consistently observed in structures of RB69pol ternary complexes.[28,29,35−38] All four water molecules are polarized and serve as extensions of protein side chains to mediate pol–DNA interactions. In contrast, the W1 water molecule was missing in the structure where dA was replaced with 3DA at position $n - 1$ of the template strand (Figure 5B). Least-squares superposition of these two structures shows that: (i) the dT/3DA base pair is completely superimposable with the dT/dA base pair at position $n - 1$ and the HB pattern and geometry of the two base pairs are almost identical (Figure 5C); (ii) the γ-hydroxyl of Y567 tilted 0.3 Å toward the main chain amide of residue G568 (Figure 5C); and (iii) the W2 water molecule shifted 1.2 Å laterally toward the Y416 side chain (Figure 5C). Thus, the 90-fold difference in the efficiency of nucleotide incorporation using different duplex DNAs (control DNA vs DNA with 3DA at position $n - 1$ of the template strand) was due to the disruption of this rigid HB network at position $n - 1$ of the template strand of the P/T duplex.

Substitution of dA with 3DA at position $n - 3$ of the primer strand did not disrupt the HB network in the minor groove of the nascent P/T duplex, as all four water molecules shown in Figure 5A can be unambiguously identified. This is consistent with the kinetics that showed that replacement of dA with 3DA at position $n - 3$ of the template strand had no effect on the kinetic parameters for nucleotide incorporation (Table 2). There is no water molecule within HB distance of C3 of 3DA at position $n - 3$ of the primer strand (Figure 6A), whereas one water molecule formed a HB with O2 of dT at position $n - 3$ of the primer strand in the structure of the ternary complex with the control DNA (Figure 6B). Clearly, this minor groove

dx.doi.org/10.1021/bi300416z | *Biochemistry* 2012, 51, 4343–4353

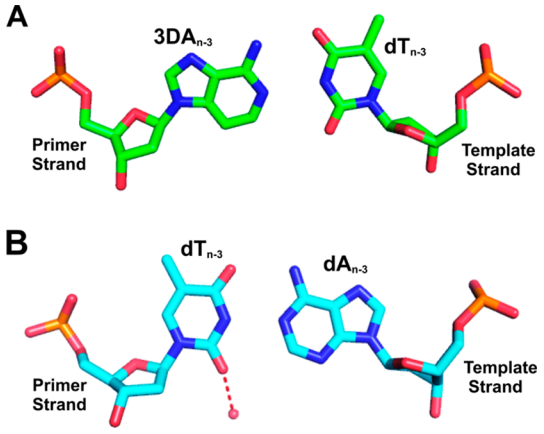

Figure 6. Minor groove HB at position $n - 3$. (A) 3DA/dT base pairs at position $n - 3$ of the P/T duplex. (B) dA/dT base pairs at position $n - 3$ of the P/T duplex in wt RB69pol with control DNA.

HB interaction at position $n - 3$ is not essential and does not affect the kinetic behavior of wt RB69pol.

Role of Minor Groove HB Interactions at Positions *n* − 1 and *n* − 2 of the Primer Strand. Because we could not obtain a dideoxy-3DA-terminated primer and because of the high $K_{d,app}$ for the incoming dNTP, we were unable to obtain a structure with 3DA at position $n - 1$ or $n - 2$ of the primer strand. However, the structure of the ternary complex with control DNA provides insight into why the dA to 3DA substitution at position $n - 1$ or $n - 2$ of the primer strand has a greater impact on incorporation efficiency than when the 3DA for dA substitution is at position $n - 1$ of the template strand. As shown in Figure 7A, the W4 water molecule formed a HB with N3 of dA at position $n - 1$ of the template strand. The orientation of the hydrogen atom from W4 is determined by the side chain of T622 and by another water molecule, W3. Replacement of dA with 3DA at position $n - 1$ of the primer strand creates a steric clash between the C3-H group of 3DA and the W4 water molecule. It is very likely that W4 will be missing just as W1 is absent in the structure where dA was replaced with 3DA at position $n - 1$ of the template strand. Because 3DA is at the primer terminus where its 3′-OH group is in a position to attack the Pα atom of an incoming dNTP, disruption of the HB network involving the minor groove of the primer strand will clearly have a greater impact on catalysis than the case in which disruption of the HB network occurs at position $n - 1$ of the template strand. This could explain why there is a 144-fold decrease in k_{pol}/K_d for the incorporation of dAMP opposite dT when 3DA is at position $n - 1$ in the primer strand and only a 90-fold decrease in k_{pol}/K_d when 3DA is at position $n - 1$ in the template strand.

The incorporation efficiency decreases by almost 3 orders of magnitude when dA is replaced with 3DA at position $n - 2$ of the primer strand. As shown in Figure 7B, the ε-amino group of K706 forms a HB with N3 of dA at position $n - 2$ of the primer strand. This is the only case that has been observed in RB69pol ternary complexes where a protein side interacts directly with N3 of a purine or O2 of a pyrimidine (which are hydrogen bond acceptors in the P/T duplex) that does not involve a water molecule. The ε-amino nitrogen of K706 is sp3-hybridized and is in perfect tetrahedral geometry (Figure 7B). It forms one HB with the carboxyl group of D621 and another with the W5 water molecule (Figure 7B). The carbonyl oxygen of D621 interacts with metal ion A via a water molecule. The adjacent residue, D623, interacts with both metal ions and is essential for catalysis. Therefore, K706 and D621 are indirectly involved in metal ion coordination, consistent with our previous mutagenesis studies.[33] The D621 to Ala replacement decreases the efficiency of incorporation of dGMP opposite dC by 10^3-fold. The K706A mutation almost eliminated pol activity. When dA was replaced with 3DA at position $n - 2$ of the primer strand, the side chain of K706 had to be repositioned to avoid a steric clash of its ε-amino group with the C3-H group of 3DA. This repositioning of K706 affects the rotomer conformation of D621 and further interferes with the coordination of metal ion A that has been proposed to activate the attacking 3′-OH of the primer terminus. Thus, any alteration of metal ion A's coordination would be expected to have a strong negative effect on catalysis. This could explain why the dA to 3DA substitution at position $n - 2$ of the primer strand resulted in a decrease in incorporation efficiency of 3 orders of magnitude.

In addition, both K706 and D621 are highly conserved in the family B pols. For example, the corresponding residues are K814 and D762 in polδ,[48] K615 and D545 in polII,[49] and K498 and D456 in ϕ29 DNA pol.[50] Interestingly, the tetrahedral geometry of the Lys ε-amino nitrogen is also conserved. As shown in Figure 8, the ε-amino group of Lys forms one HB with the carboxyl group of Asp, one HB with a water molecule, and one HB with either N3 of a purine or O2 of a pyrimidine. In contrast, no HB is observed between K706 and D621 in the apo structure of RB69pol.[11] For these reasons, we propose that the minor groove HB interaction at position $n - 2$ of the primer strand in RB69pol is essential for the correct orientation of K706 and D621 side chains and for the coordination of metal ion A. All these features are conserved in family B pols.

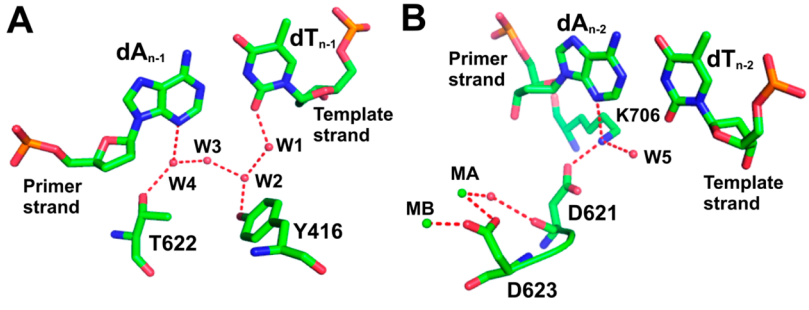

Figure 7. Minor groove HB at positions $n - 1$ and $n - 2$. (A) HB network and dA/dT base pair at the position $n - 1$ of the P/T duplex. (B) HB interactions between K706 and dA at position $n - 2$ of the primer strand and between K706 and D621.

dx.doi.org/10.1021/bi300416z | *Biochemistry* 2012, 51, 4343−4353

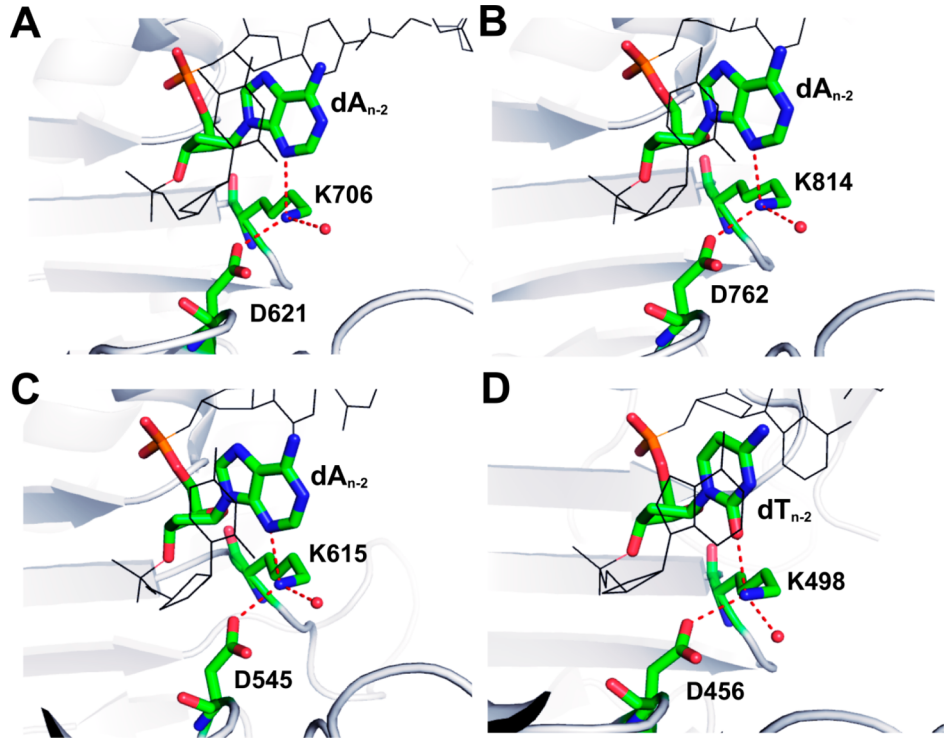

Figure 8. Conserved tetrahedral geometry of the Lys ε-amino nitrogen in (A) RB69pol, (B) polδ, (C) polII, and (D) ϕ29 DNA pol.

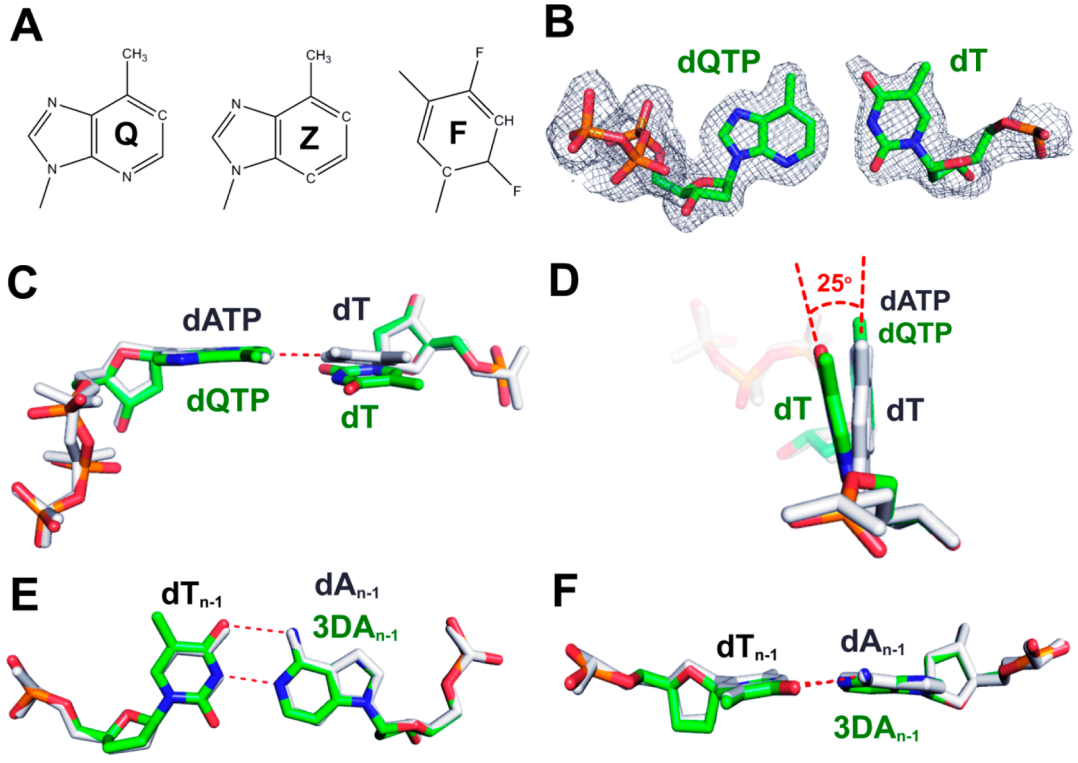

Figure 9. dQTP/dT-containing ternary complex of the RB69pol triple mutant. (A) Chemical structures of Q, Z, and F. (B) Final $2F_o - F_c$ electron density map for dQTP and dT contoured at 1.6σ. (C) Superposition of the dQTP- and dT-containing ternary complex of the RB69pol triple mutant with the dATP/dT-containing ternary complex of wt RB69pol. (D) Orthogonal view of panel C. (E) Superposition of the structure with control DNA with the structure with 3DA at position $n - 1$ of the template strand. (F) Orthogonal view of panel E.

Probing Minor Groove HB Interactions with Nucleotide Analogues. Since Steitz[51] pointed out that the minor groove HB interactions between protein side chains and N3 of purines or O2 of pyrimidines are important for replication fidelity, numerous kinetic and structural studies have been conducted on DNA pols from different families.[26,52−56] In particular, various purine and pyrimidine analogues have been used to address the crucial role of minor groove HBs in DNA

dx.doi.org/10.1021/bi300416z | *Biochemistry* 2012, 51, 4343−4353

replication. Morales et al were the first to use Q, Z, and F (Figure 9A) to study minor groove interactions between pol and DNA.[26,55,57] Q and Z are nonpolar purine analogues, and F was assumed to be a nonpolar pyrimidine analogue. According to Morales's steady-state kinetics studies,[26] Klenow fragment (KF) was able to bypass a dQ/dF pair 300-fold more efficiently than a dZ/dF pair. Because dZ lacks a minor groove HB acceptor at the C3 position of the purine ring, Morales et al. concluded that a single minor groove interaction in the primer strand with KF was responsible for the 300-fold decrease in primer extension efficiency.[26] Nevertheless, the question of whether Q, Z, or F was an appropriate nucleotide analogue for studying minor groove HB interactions remained. We raise this issue because our recent report on dF-containing RB69 ternary complexes showed that dF can actually form HBs and thus F cannot be classified as a strictly nonpolar isostere of dT.[28,29]

In addition, we determined the structure of a dQTP- and dT-containing ternary complex of RB69pol at 2.0 Å (data collection and structure refinement statistics of this structure are provided as Supporting Information). As shown in Figure 9B, there is no direct interbase HB between dQTP and dT. Superimposition of this structure with the dATP/dT-containing ternary complex of wt RB69pol shows that dT tilts 25° toward residue S565 to avoid a steric clash between dQTP's C1-H group and dT's N3-H group (Figure 9C,D). As a result, dQTP and dT are not in the same plane because of the interbase repulsive interaction. We also expect that dQ and dT will not be in the same plane when they are at position $n - 1$ in a P/T duplex, nor will the dQ/dF or dZ/dF base pair. The resulting distortion of the DNA duplex at the P/T junction would be expected to cause misalignment between the 3′-hydroxyl group at the primer terminus and the α-phosphorus atom of the incoming dNTP. Thus, the decrease in incorporation efficiency is caused not only by the absence of minor groove HB interactions but also by distortion of the base pair at position $n - 1$ of the P/T duplex. Because N3 was replaced with C3 in dZ, the dZ/dF base pair may be more tilted or distorted at the P/T junction than the dQ/dF base pair. Thus, it is very likely that the lack of minor groove−pol HB interactions at the primer/template junction is not the sole reason for the 300-fold difference in bypass efficiency between dQ/dF and dZ/dF base pairs. In contrast, the structure of the ternary complex with dT and 3DA at position $n - 1$ of the template strand can be superimposed perfectly on the ternary complex containing a dT/dA base pair at position $n - 1$ of the template strand in the P/T duplex (Figure 9E). 3DA and dT are in the same plane just like dT/dA (Figure 9F). This illustrates why 3DA is a better purine analogue than Z or Q for probing minor groove HB interactions between N3 of a purine and a pol. The observed 90-fold difference in the efficiency of incorporation of correct dNMP past P/Ts containing a dT/dA or dT/3DA base-pair at the primer termini was due solely to the disruption of the minor groove HB network involving position $n - 1$ of the template strand.

Hendrickson et al.[56] used 3-deaza-2-deoxyadenosine triphosphate (c^3dATP) to probe minor groove interactions in three family A pols and three family B pols. However, their primer extension assays did not provide results that allowed quantitative evaluation of minor groove HB interactions with the pols. In addition, the three family B pols chosen were all thermostable pols with optimal temperatures for extension of ~72 °C. Thus, it is not clear that their findings would apply to the majority of family B pols. In addition, pyrimidine analogues lacking the 2-keto group, such as 2-amino-5-(2′-deoxy-β-D-ribofuranosyl)pyridine 5′-triphosphate (d*CTP) and 5-(2′-deoxy-β-D-ribofuranosyl)-3-methyl-2-pyridone 5′-triphosphate (d*TTP), were found to inhibit DNA pol activity.[54] It should be noted that no study has been conducted on the influence of the pyrimidine 2-keto group at position $n - 1$ of a DNA duplex where it has been shown that pol−minor groove HB interactions are conserved in family A pols.[15−17] McCain et al.[58] determined steady-state and pre-steady-state kinetic parameters for DNA synthesis by KF using 10 different duplexes in which 3-deazaguanine (3DG) was placed at different positions. They found that R668 forms a HB fork between the minor groove of the primer terminus and the deoxyribose ring oxygen of the incoming dNTP. Because KF is a model family A pol, in our study of minor groove HB interactions using 3DA and RB69pol, a model family B pol complements the results of McCain et al.[58]

In summary, we have shown that minor groove HB interactions are essential for efficient nucleotide incorporation. For example, the minor groove HB interaction mediated by one water molecule between position $n - 1$ of the template strand and Y567 is critical for efficient nucleotide incorporation, and the minor groove HB interaction at position $n - 2$ of the primer strand in RB69pol is essential for correctly orienting the K706 and D621 side chains and optimizing coordination of metal ion A with D623 and D411. The absence of a single minor groove HB interaction can result in an up to 10^3-fold decrease in incorporation efficiency. In addition, our fluorescence lifetime measurements have shown that minor groove HBs help to stabilize the P/T duplex in the pol domain. Our structures show that 3DA is an ideal analogue for probing minor groove HB interactions between pol and nucleobases in duplex DNA.

■ ASSOCIATED CONTENT

Supporting Information

One table and three figures. This material is available free of charge via the Internet at http://pubs.acs.org.

■ AUTHOR INFORMATION

Corresponding Author

*SHM CE-14, Department of Molecular Biophysics and Biochemistry, Yale University, New Haven, CT 06520-8114. Telephone: (203) 785-4599. Fax: (203) 785-7979. E-mail: william.konigsberg@yale.edu.

Funding

This work was supported by National Institutes of Health Grant RO1-GM063276−09 (to W.H.K.) and by SCSB-GIST (to J.W.).

Notes

The authors declare no competing financial interest.

■ ACKNOWLEDGMENTS

We thank the staff of NE-CAT beamline 24-ID-E at the Advanced Photon Source of Argonne National Laboratory.

■ ABBREVIATIONS

pol, polymerase; exo, exonuclease; RB69pol, RB69 DNA polymerase; NBP, nascent base pair binding pocket; P/T, primer/template; W−C, Watson−Crick; wt, wild type; HB, hydrogen bonding or hydrogen bond; KF, Klenow fragment; tC°, 1,3-diaza-2-oxophenoxazine; 3DA, 3-deaza-2′-deoxyadeno-

sine; 3DG, 3-deaza-2′-deoxyguanosine; 2AP, 2-aminopurine; F, 2,4-difluorotoluene deoxynucleoside; Z, 4-methylbenzimidazole deoxynucleoside; Q, 9-methyl-1*H*-imidazo[4,5-*b*]pyridine; dQTP, 9-methyl-1*H*-imidazo[4,5-*b*]pyridine triphosphate; c^3dATP, 3-deaza-2-deoxyadenosine triphosphate; PEG 350 MME, polyethylene glycol 350 monomethyl ether; K_d, dissociation constant for the P/T−pol binary complex; $K_{d,app}$, dNTP concentration that gives half of the maximal rate.

REFERENCES

(1) Kunkel, T. A., and Bebenek, K. (1988) Recent studies of the fidelity of DNA synthesis. *Biochim. Biophys. Acta 951*, 1−15.

(2) Drake, J. W. (1991) A constant rate of spontaneous mutation in DNA-based microbes. *Proc. Natl. Acad. Sci. U.S.A. 88*, 7160−7164.

(3) Echols, H., and Goodman, M. F. (1991) Fidelity mechanisms in DNA replication. *Annu. Rev. Biochem. 60*, 477−511.

(4) Joyce, C. M., and Benkovic, S. J. (2004) DNA polymerase fidelity: Kinetics, structure, and checkpoints. *Biochemistry 43*, 14317−14324.

(5) Kunkel, T. A. (2004) DNA replication fidelity. *J. Biol. Chem. 279*, 16895−16898.

(6) Loeb, L. A., and Kunkel, T. A. (1982) Fidelity of DNA synthesis. *Annu. Rev. Biochem. 51*, 429−457.

(7) Kunkel, T. A., and Bebenek, K. (2000) DNA replication fidelity. *Annu. Rev. Biochem. 69*, 497−529.

(8) Kunkel, T. A., and Erie, D. A. (2005) DNA mismatch repair. *Annu. Rev. Biochem. 74*, 681−710.

(9) Schweitzer, B. A., and Kool, E. T. (1994) Aromatic Nonpolar Nucleosides as Hydrophobic Isosteres of Pyrimidine and Purine Nucleosides. *J. Org. Chem. 59*, 7238−7242.

(10) Doublie, S., Tabor, S., Long, A. M., Richardson, C. C., and Ellenberger, T. (1998) Crystal structure of a bacteriophage T7 DNA replication complex at 2.2 Å resolution. *Nature 391*, 251−258.

(11) Franklin, M. C., Wang, J., and Steitz, T. A. (2001) Structure of the replicating complex of a pol α family DNA polymerase. *Cell 105*, 657−667.

(12) Johnson, S. J., and Beese, L. S. (2004) Structures of mismatch replication errors observed in a DNA polymerase. *Cell 116*, 803−816.

(13) Kool, E. T., and Sintim, H. O. (2006) The difluorotoluene debate: A decade later. *Chem. Commun.*, 3665−3675.

(14) Seeman, N. C., Rosenberg, J. M., and Rich, A. (1976) Sequence-specific recognition of double helical nucleic acids by proteins. *Proc. Natl. Acad. Sci. U.S.A. 73*, 804−808.

(15) Eom, S. H., Wang, J., and Steitz, T. A. (1996) Structure of Taq polymerase with DNA at the polymerase active site. *Nature 382*, 278−281.

(16) Kiefer, J. R., Mao, C., Braman, J. C., and Beese, L. S. (1998) Visualizing DNA replication in a catalytically active *Bacillus* DNA polymerase crystal. *Nature 391*, 304−307.

(17) Li, Y., Korolev, S., and Waksman, G. (1998) Crystal structures of open and closed forms of binary and ternary complexes of the large fragment of *Thermus aquaticus* DNA polymerase I: Structural basis for nucleotide incorporation. *EMBO J. 17*, 7514−7525.

(18) Spratt, T. E. (2001) Identification of hydrogen bonds between *Escherichia coli* DNA polymerase I (Klenow fragment) and the minor groove of DNA by amino acid substitution of the polymerase and atomic substitution of the DNA. *Biochemistry 40*, 2647−2652.

(19) Singh, K., and Modak, M. J. (2003) Presence of 18-Å long hydrogen bond track in the active site of *Escherichia coli* DNA polymerase I (Klenow fragment). Its requirement in the stabilization of enzyme-template-primer complex. *J. Biol. Chem. 278*, 11289−11302.

(20) Thompson, E. H., Bailey, M. F., van der Schans, E. J., Joyce, C. M., and Millar, D. P. (2002) Determinants of DNA mismatch recognition within the polymerase domain of the Klenow fragment. *Biochemistry 41*, 713−722.

(21) Wang, J., Sattar, A. K., Wang, C. C., Karam, J. D., Konigsberg, W. H., and Steitz, T. A. (1997) Crystal structure of a pol α family replication DNA polymerase from bacteriophage RB69. *Cell 89*, 1087−1099.

(22) Polesky, A. H., Steitz, T. A., Grindley, N. D., and Joyce, C. M. (1990) Identification of residues critical for the polymerase activity of the Klenow fragment of DNA polymerase I from *Escherichia coli*. *J. Biol. Chem. 265*, 14579−14591.

(23) Polesky, A. H., Dahlberg, M. E., Benkovic, S. J., Grindley, N. D., and Joyce, C. M. (1992) Side chains involved in catalysis of the polymerase reaction of DNA polymerase I from *Escherichia coli*. *J. Biol. Chem. 267*, 8417−8428.

(24) Joyce, C. M., and Steitz, T. A. (1994) Function and structure relationships in DNA polymerases. *Annu. Rev. Biochem. 63*, 777−822.

(25) Yang, G., Lin, T., Karam, J., and Konigsberg, W. H. (1999) Steady-state kinetic characterization of RB69 DNA polymerase mutants that affect dNTP incorporation. *Biochemistry 38*, 8094−8101.

(26) Morales, J. C., and Kool, E. T. (1999) Minor Groove Interactions between Polymerase and DNA: More Essential to Replication than Watson-Crick Hydrogen Bonds? *J. Am. Chem. Soc. 121*, 2323−2324.

(27) Xia, S., Vashishtha, A., Eom, S. H., Wang, J., and Konigsberg, W. (2012) Contribution of partial charge interactions and base-stacking to the efficiency of primer-extension at and beyond abasic sites in DNA. *Biochemistry*, (in press).

(28) Xia, S., Konigsberg, W. H., and Wang, J. (2011) Hydrogen-bonding capability of a templating difluorotoluene nucleotide residue in an RB69 DNA polymerase ternary complex. *J. Am. Chem. Soc. 133*, 10003−10005.

(29) Xia, S., Eom, S. H., Konigsberg, W. H., and Wang, J. (2012) Structural Basis for Differential Insertion Kinetics of dNMPs Opposite a Difluorotoluene Nucleotide Residue. *Biochemistry 51*, 1476−1485.

(30) Braithwaite, D. K., and Ito, J. (1993) Compilation, alignment, and phylogenetic relationships of DNA polymerases. *Nucleic Acids Res. 21*, 787−802.

(31) Yang, G., Franklin, M., Li, J., Lin, T. C., and Konigsberg, W. (2002) Correlation of the kinetics of finger domain mutants in RB69 DNA polymerase with its structure. *Biochemistry 41*, 2526−2534.

(32) Yang, G., Franklin, M., Li, J., Lin, T. C., and Konigsberg, W. (2002) A conserved Tyr residue is required for sugar selectivity in a Pol α DNA polymerase. *Biochemistry 41*, 10256−10261.

(33) Zakharova, E., Wang, J., and Konigsberg, W. (2004) The activity of selected RB69 DNA polymerase mutants can be restored by manganese ions: The existence of alternative metal ion ligands used during the polymerization cycle. *Biochemistry 43*, 6587−6595.

(34) Zhang, H., Beckman, J., Wang, J., and Konigsberg, W. (2009) RB69 DNA polymerase mutants with expanded nascent base-pair-binding pockets are highly efficient but have reduced base selectivity. *Biochemistry 48*, 6940−6950.

(35) Wang, M., Xia, S., Blaha, G., Steitz, T. A., Konigsberg, W. H., and Wang, J. (2011) Insights into base selectivity from the 1.8 Å resolution structure of an RB69 DNA polymerase ternary complex. *Biochemistry 50*, 581−590.

(36) Xia, S., Wang, M., Blaha, G., Konigsberg, W. H., and Wang, J. (2011) Structural Insights into Complete Metal Ion Coordination from Ternary Complexes of B Family RB69 DNA Polymerase. *Biochemistry 50*, 9114−9124.

(37) Xia, S., Wang, M., Lee, H. R., Sinha, A., Blaha, G., Christian, T., Wang, J., and Konigsberg, W. (2011) Variation in mutation rates caused by RB69pol fidelity mutants can be rationalized on the basis of their kinetic behavior and crystal structures. *J. Mol. Biol. 406*, 558−570.

(38) Xia, S., Eom, S. H., Konigsberg, W. H., and Wang, J. (2012) Bidentate and tridentate metal-ion coordination states within ternary complexes of RB69 DNA polymerase. *Protein Sci. 21*, 447−451.

(39) Reha-Krantz, L. J., Hariharan, C., Subuddhi, U., Xia, S., Zhao, C., Beckman, J., Christian, T., and Konigsberg, W. (2011) Structure of the 2-aminopurine-cytosine base pair formed in the polymerase active site of the RB69 Y567A-DNA polymerase. *Biochemistry 50*, 10136−10149.

(40) Otwinowski, Z., and Minor, W. (1997) Processing of X-ray diffraction data collected in oscillation mode. *Methods Enzymol. 276*, 307−326.

(41) McCoy, A. J., Grosse-Kunstleve, R. W., Adams, P. D., Winn, M. D., Storoni, L. C., and Read, R. J. (2007) Phaser crystallographic software. *J. Appl. Crystallogr. 40*, 658−674.
(42) Murshudov, G. N., Vagin, A. A., and Dodson, E. J. (1997) Refinement of macromolecular structures by the maximum-likelihood method. *Acta Crystallogr. D53*, 240−255.
(43) Emsley, P., and Cowtan, K. (2004) Coot: Model-building tools for molecular graphics. *Acta Crystallogr. D60*, 2126−2132.
(44) *The PyMOL Molecular Graphics System*, version 1.2r3pre (2011) Schrodinger, LLC, New York.
(45) Borjesson, K., Sandin, P., and Wilhelmsson, L. M. (2009) Nucleic acid structure and sequence probing using fluorescent base analogue tC^{O}. *Biophys. Chem. 139*, 24−28.
(46) Preus, S., Borjesson, K., Kilsa, K., Albinsson, B., and Wilhelmsson, L. M. (2010) Characterization of nucleobase analogue FRET acceptor tCnitro. *J. Phys. Chem. B 114*, 1050−1056.
(47) Xia, S., Beckman, J., Wang, J., and Konigsberg, W. (2012) Using fluorescent cytosine analogue tCo to probe the effect of Y567 to Ala substitution on the pre-insertion steps of dNMP incorporation by RB69 DNA polymerase. *Biochemistry*, (in press).
(48) Swan, M. K., Johnson, R. E., Prakash, L., Prakash, S., and Aggarwal, A. K. (2009) Structural basis of high-fidelity DNA synthesis by yeast DNA polymerase *δ*. *Nat. Struct. Mol. Biol. 16*, 979−986.
(49) Wang, F., and Yang, W. (2009) Structural insight into translesion synthesis by DNA Pol II. *Cell 139*, 1279−1289.
(50) Berman, A. J., Kamtekar, S., Goodman, J. L., Lazaro, J. M., de Vega, M., Blanco, L., Salas, M., and Steitz, T. A. (2007) Structures of *ϕ*29 DNA polymerase complexed with substrate: The mechanism of translocation in B-family polymerases. *EMBO J. 26*, 3494−3505.
(51) Steitz, T. A. (1990) Structural studies of protein-nucleic acid interaction: The sources of sequence-specific binding. *Q. Rev. Biophys. 23*, 205−280.
(52) Cosstick, R., Li, X., Tuli, D. K., Williams, D. M., Connolly, B. A., and Newman, P. C. (1990) Molecular recognition in the minor groove of the DNA helix. Studies on the synthesis of oligonucleotides and polynucleotides containing 3-deaza-2′-deoxyadenosine. Interaction of the oligonucleotides with the restriction endonuclease EcoRV. *Nucleic Acids Res. 18*, 4771−4778.
(53) Spratt, T. E. (1997) Klenow fragment-DNA interaction required for the incorporation of nucleotides opposite guanine and O6-methylguanine. *Biochemistry 36*, 13292−13297.
(54) Guo, M. J., Hildbrand, S., Leumann, C. J., McLaughlin, L. W., and Waring, M. J. (1998) Inhibition of DNA polymerase reactions by pyrimidine nucleotide analogues lacking the 2-keto group. *Nucleic Acids Res. 26*, 1863−1869.
(55) Morales, J. C., and Kool, E. T. (2000) Varied Molecular Interactions at the Active Sites of Several DNA Polymerases: Nonpolar Nucleoside Isosteres as Probes. *J. Am. Chem. Soc. 122*, 1001−1007.
(56) Hendrickson, C. L., Devine, K. G., and Benner, S. A. (2004) Probing minor groove recognition contacts by DNA polymerases and reverse transcriptases using 3-deaza-2′-deoxyadenosine. *Nucleic Acids Res. 32*, 2241−2250.
(57) Morales, J. C., and Kool, E. T. (1998) Efficient replication between non-hydrogen-bonded nucleoside shape analogs. *Nat. Struct. Biol. 5*, 950−954.
(58) McCain, M. D., Meyer, A. S., Schultz, S. S., Glekas, A., and Spratt, T. E. (2005) Fidelity of mispair formation and mispair extension is dependent on the interaction between the minor groove of the primer terminus and Arg668 of DNA polymerase I of *Escherichia coli*. *Biochemistry 44*, 5647−5659.